Cis- and *Trans*-acting Functions Required for Endocytosis of the Yeast Pheromone Receptors

Nicholas G. Davis, Joseph L. Horecka, and George F. Sprague, Jr.

Institute of Molecular Biology and Department of Biology, University of Oregon, Eugene, Oregon 97403

Abstract. The *Saccharomyces cerevisiae* a-factor receptor (STE3) is subject to two modes of endocytosis: a constitutive process that occurs in the absence of ligand and a regulated process that is triggered by binding of ligand. Both processes result in delivery of the receptor to the vacuole for degradation. Receptor mutants deleted for part of the COOH-terminal cytoplasmic domain are disabled for constitutive, but not ligand-dependent internalization. *Trans*-acting mutants that impair constitutive endocytosis have been isolated. One of these, *ren1-1*, is blocked at a late step in the endocytic pathway, as receptor accumulates in a pre-vacuolar endosome-like compartment. *REN1* is identical to *VPS2*, a gene required for delivery of newly synthesized vacuolar enzymes to the vacuole. Based on this identity, we suggest a model in which the transport pathways to the vacuole—the endocytic pathway and the vacuolar biogenesis pathway—merge at an intermediate endocytic compartment. As receptor also accumulates at the surface of *ren1* cells, receptor may recycle from the putative endosome to the surface, or REN1 may also be required to carry out an early step in endocytosis.

ENDOCYTOSIS of cell surface receptors plays a vital role in cell physiology. Endocytosis of some receptors, for example, the transferrin or LDL receptors, is the first step in the delivery of essential nutrients to the cell. Endocytosis of other receptors, particularly hormone receptors, serves to control receptor abundance and therefore the cell's sensitivity to hormone. Most receptor-mediated endocytosis is thought to occur via clustering of receptors at clathrin-coated pits, which pinch off from the surface giving coated vesicles. Once internalized, receptor and ligand pass through early and late endosomal compartments. From these compartments the endocytic pathway branches, allowing either recycling back to the cell surface or delivery to the lysosome for hydrolysis (for reviews see Goldstein et al., 1985; Schlessinger, 1988; Gruenberg and Howell, 1989; Kornfeld and Melman, 1989; Griffiths and Gruenberg, 1991; Pfeffer, 1992).

Many features of endocytosis, including the requirement for initial association with clathrin pits, vary among receptor types. Some receptors, for example the low-density lipoprotein (LDL)[1] receptor, associate spontaneously with the pits and are internalized at a constant rate irrespective of their liganded state (Anderson et al., 1978). Other receptors, for example the EGF receptor, associate with clathrin pits only when bound by ligand, and thus it is the ligand binding event that triggers endocytosis (Schlessinger et al., 1978; Maxfield et al., 1978). Receptor types also have different destinies once internalized. LDL and its receptor dissociate in the early endosome. The receptor is then recycled to the surface while the ligand is delivered to the lysosome for hydrolysis (Basu et al., 1981). On the other hand, both EGF and its receptor are delivered to and degraded in the lysosome (Carpenter and Cohen, 1976).

Although there is a sophisticated picture of the initial events of endocytosis and the subsequent membrane traffic, the mechanisms that underlie and regulate the processes are poorly understood. In particular, aside from clathrin and clathrin-associated proteins termed adaptins (Pearse and Robinson, 1984), which are involved in coated pit formation, and rab proteins, a class of GTP-binding proteins some of which have been found associated with early and late endosomes (Chavrier et al., 1990; van der Slijs et al., 1991, 1992; Bucci et al., 1992), the molecules that catalyze and control each step of the endocytic pathway are unknown. With the expectation that a genetic analysis would contribute to the identification of such molecules, we have investigated the internalization of the pheromone receptors of the yeast *Saccharomyces cerevisiae* and have begun to isolate mutants defective for internalization. Pheromone receptors enable cell-cell communication as a prelude to mating of the two haploid cell types, a and α (Herskowitz, 1989). Each cell type secretes a unique peptide pheromone—a-factor by a cells and α-factor by α cells—and expresses at its surface a receptor for the pheromone secreted by the other cell type. Binding of pheromone to its cognate receptor activates an in-

1. *Abbreviations used in this paper:* ALP, alkaline phosphatase; CPY, carboxypeptidase; DB, digestion buffer; LDL, low-density lipoprotein; SB, sample buffer; *vps*, vacuolar protein sorting.

tracellular signal transduction pathway that leads to the physiological alterations that permit mating.

The pheromone receptors are members of a large family of G protein–coupled receptors initially defined by the β-adrenergic receptor and the rhodopsins (Dohlman et al., 1991). Although receptors of this family often show little sequence identity, they do share structural similarities. In particular, they are characterized by an NH_2-terminal domain with seven hydrophobic, presumably membrane-spanning segments followed by a hydrophilic COOH-terminal domain oriented toward the cytoplasm. In cases where it has been examined, deletion of the bulk of the COOH-terminal domain does not interfere with ligand binding or G protein coupling, indicating that the seven transmembrane segment domain suffices for these functions. Deletion of the receptor COOH-terminal domain results in a heightened and prolonged response to ligand, implying that this domain functions to attenuate receptor activity (Konopka et al., 1988; Reneke et al., 1988; Dohlman et al., 1991; C. Boone, N. Davis, and G. Sprague, manuscript submitted for publication).

Endocytosis of the seven transmembrane segment receptor family has not been extensively studied. Treatment of animal cells with β-adrenergic agonists results in a rapid loss of surface binding sites, implying that the receptor has been internalized (Benovic et al., 1988). Whether these receptors associate with clathrin pits has not been investigated. Studies with yeast have suggested that the α-factor receptor is also likely subject to endocytosis. First, treatment with α-factor results in the loss of surface binding sites (Jenness and Spatrick, 1986). Second, the α-factor ligand is internalized and degraded by a pathway that involves an intracellular vesicular compartment, perhaps an endosome (Jenness and Spatrick, 1986; Chvatchko et al., 1986; Singer and Riezman, 1990). Because degradation of α-factor requires vacuolar protease activity, it is presumed that the ligand is delivered to the vacuole, an organelle equivalent to the lysosome. Third, disruption of the yeast clathrin heavy chain gene (Payne and Schekman, 1985; Lemmon and Jones, 1987) reduces the rate of α-factor uptake (Payne et al., 1988). Recently several mutants that block either the uptake or degradation of α-factor have been isolated (Wichmann et al., 1992; Raths et al., 1993). However, for neither wild-type cells nor these endocytosis mutants has the fate of the receptor itself been investigated.

In this paper we demonstrate endocytosis of the pheromone receptors by examining the receptor protein directly. We focus on the a-factor receptor and measure its stability and location in the presence and absence of pheromone. We conclude that this receptor is subject to two apparently discrete modes of endocytosis, both of which deliver the protein to the vacuole for degradation. One mode is constitutive, occurring in the absence of a-factor ligand, whereas the second mode is triggered by ligand. Receptor mutants deleted for part of the COOH-terminal domain are defective for constitutive endocytosis but normal for ligand-stimulated endocytosis. We also report the isolation of *trans*-acting mutations that block receptor endocytosis or subsequent steps in the endocytic pathway (*ren* mutations). Our characterization suggests that the wild-type REN1 product acts relatively late in the endocytic pathway, as internalized receptor accumulates in a prevacuolar endosome-like compartment in *ren1* mutants. Based on the identity of *ren1* with *vps2*, a class E *vps* mutant (defective in vacuolar protein sorting), we suggest a model in which the two transport pathways to the vacuole—endocytic transport and the transport of newly synthesized vacuolar enzymes—merge at an intermediate endosomal compartment before vacuolar delivery.

Materials and Methods

Plasmids

pSL552 (Bender and Sprague, 1986) has *STE3* under the control of the *GAL1* promoter carried on YCp50. pSL1922 is the same as pSL552 except for the *Δ365* mutation, a deletion of 310-bp extending from the *STE3* SalI site to the PstI site. In-frame fusion required addition of a 12-bp SalI linker to the PstI end from which the 3′ overhang had been removed by treatment with the Klenow fragment of DNA polymerase. This resulted in the insertion of an arginine codon between codon *365* and the two COOH-terminal *STE3* codons.

pSL2099 has the c-*myc* 9E10 epitope fused to the COOH terminus of *GAL1-STE3*, carried on the *LEU2* CEN/ARS vector pRS315 (Sikorski and Hieter, 1989). 18 new codons, including the c-*myc* epitope (Evan et al., 1985) were inserted in-frame at the *STE3* PstI site disrupting only the three final *STE3* residues; the resulting COOH-terminal 25 residues of this fusion protein are now ENTGSKMEQKLISEEDLFLDRGP (protein sequence from *STE3* is underlined).

Strains

SY1793 is a *MATα mfa1Δ mfa2Δ* derivative of Sc252 (Whiteway et al., 1990), created by *GAL-HO* promoted mating type interconversion and two-step gene replacement at the *MFA* loci (Table I; Jensen and Herskowitz, 1984; Rothstein, 1991). In addition, the pheromone-dependent *FUS1* UAS replaced the *HIS3* UAS at the *HIS3* locus (Stevenson et al., 1992). The deletion endpoints of *mfa1Δ* and *mfa2Δ* are the same as for previously reported disruption alleles, *mfa1::LEU2* and *mfa2::URA3* (Michaelis and Herskowitz, 1988).

SY1817 is a *ste3Δ* derivative of SY1793 made by two-step gene replacement. This deletion removes the *STE3* coding sequence and UAS, and extends from an RsaI site 417 bp upstream of the AUG, to a SacI site 111 bp downstream of the stop codon (Hagen et al., 1986). SY1884 is a *pep4Δ* derivative of SY1817 (Rothman et al., 1986). *GAL1-STE3* (SY2152) or *GAL1-STE3Δ365* (SY2132) were constructed by two-step gene replacement at the *STE3* locus of SY1884.

SY1369 is a Met^+ revertant of YY1152 (Clark et al., 1988). *ste3Δ* (SY1372), *GAL1-STE3* (SY1426) and *GAL1-STE3Δ365* (SY1610) alleles were inserted into the chromosome of SY1369 by one step replacement of *ste3::URA3*, selecting for Ura^- derivatives with 5-fluoro-orotic acid (Boeke et al., 1984). SY1683 is a *pep4Δ* derivative of SY1372 (Rothman et al., 1986). SY1553 is a *MATa* version of SY1426 made via an *HO*-induced mating type switch. SY1616 is a *pep4::URA3* derivative of SY1426 made by one step gene replacement (Rothman et al., 1986). SY1498 is a *mat1* derivative of SY1426 carrying XhoI linker insertion mutation 23 (Tatchell et al., 1981).

ren1-1 was isolated in a *mat1* cell carrying the *MATα* plasmid pSL602 (Bender and Sprague, 1986). Loss of pSL602 yielded SY1534. *MATα* (SY1560) and *MATa*(SY1614) derivatives of SY1534 were created by *HO*-promoted mating type interconversion. SY1650 is a *MATα ren1-1* segregant derived from a backcross of SY1614 to SY1426. The *GAL1-STE3* constructs in SY1426 and SY1560 were replaced with the natural *STE3* promoter by the two step method yielding SY1574 and SY1579, respectively.

SY1675 is *MATa GAL1-STE3 pep4::URA3* segregant from a cross between SY1553 and SY1616. SY1744 and SY1745 are *MATα STE3 pep4::URA3* and *MATa STE3* segregants of a cross between SY1574 and SY1675.

The *GAL1-STE3Δ365*(c-*myc*) strain SY2559 was constructed by two step gene replacement at the *STE3* locus of SY1683. The C-terminus of STE3 Δ365 construct (described for pSL1922) was tagged at its SalI site with the in-frame insertion of 18 new codons including the c-*myc* 9E10 epitope (Evan et al., 1985) between Asp 365 and Gly 469. The resulting C-terminal 25 residues of this fusion protein are now YVDGSKMEQKLISEEDLFLDRGP (protein sequence from *STE3* is underlined).

SY1745 was made *GAL1-STE2* via the two step method yielding SY1960;

for this *STE2* allele, a 326-bp *GAL1,10* UAS fragment substitutes for the 360-bp HindIII fragment that includes the natural *STE2* UAS. SY2029 is a *MAT***a** *GAL1–STE2 pep4::URA3* segregant of a cross between SY1744 and SY1960. SY2041 is a *MAT***a** *GAL1–STE2 ren1-1* segregant of a cross between SY1579 and SY1960.

Antisera

Rabbit antiserum raised against TrpE–STE3 fusion protein (Clark et al., 1988) was affinity-purified using the fusion protein antigen coupled to CNBr-activated Sepharose 4B (Sigma Immunochemicals, St. Louis, MO; Roberts et al., 1991). This fusion has the COOH-terminal 183 residues of STE3. Another aliquot of this antiserum was affinity-purified using a TrpE-STE3Δ365 fusion.

Rabbit antiserum against the STE2 protein was a generous gift from James Konopka (Konopka et al., 1988). Affinity-purified alkaline phosphatase (ALP) rabbit antiserum was generously provided by Chris Raymond (University of Oregon). Mouse mAb-1 reactive with the c-*myc* epitope was purchased from Oncogene Science Inc. (Manhasset, NY).

Cell Labeling and Immune Precipitation

Exponential cultures of cells (2×10^7/ml) growing at 30°C in supplemented minimal medium lacking methionine and cysteine were pulse-labeled for 10 min with [^{35}S]methionine (0.5 mCi/ml) and then chased with subsequent addition methionine and cysteine to 50 μg/ml. To prepare protein extracts, 250 μl of the labeled cell culture was collected by centrifugation, suspended in 150 μl digestion buffer (DB; 1.4 M sorbitol, 25 mM Tris/Cl pH 7.5, 10 mM sodium azide, 10 mM potassium fluoride, 2 mM MgCl) with 0.3% β-mercaptoethanol and oxalyticase (Enzogenetics, Corvallis, OR) at 600 U/ml, and incubated at 30°C for 30 min. Spheroplasts were pelleted, suspended in SDS-PAGE sample buffer (SB; 40 mM Tris/Cl pH 6.8, 8 M urea, 0.1 mM EDTA, 1% β-mercaptoethanol) with 2.5% SDS, and then lysed at 100°C for 5 min. Protein extract was diluted 20-fold into immune precipitation buffer (IP; 10 mM Tris/Cl pH 8.0, 0.1% Triton X-100, 2 mM EDTA) with 0.5 mM PMSF, 1 μg/ml leupeptin, 1 μg/ml pepstatin and 0.5% IgG-Sorb (The Enzyme Center, Malden, MA). After 15 min at 0°C, IgGSorb was removed by centrifugation and STE3 antiserum was added to the supernatant at 1:200. After 1 h at 0°C, IgGSorb was added to 0.5%. After 30 min further incubation, immune complexes were washed four times with IP plus 0.1% SDS. Precipitated protein was eluted from the antibody-IgGSorb complex by suspension in SB with 5% SDS and incubation at 100°C for 5 min. The protein was then subjected to SDS-PAGE.

Immunoblots

To prepare protein extracts for Western blotting, 1.5×10^8 log-phase cells grown at 30°C were pelleted, immediately frozen on dry ice, and then stored at −70°C. Cell pellets were thawed by suspension in 100 μl of SB with 5% SDS and transferred to a 1.5 ml microfuge tube containing an 80 μl volume of glass beads. After being vortexed for 10 min, samples were incubated at 37°C for 10 min. 25 μl of SDS-PAGE sample buffer was added, samples were vortexed for 2 min, and then 10 μl of the supernatant fraction from a 5-min microfuge spin was subjected to electrophoresis. Protein was transferred to nitrocellulose and treated with antibody. For STE3 detection, antiserum that had been affinity purified against the large TrpE–STE3 fusion was used at 1:10,000. For STE2, antiserum was used at 1:500 dilution. Primary antibodies were detected with an HRP-conjugated anti-rabbit IgG second antibody followed by the ECL chemiluminescent system (Amersham Corp., Arlington Heights, IL).

Susceptibility to External Proteases

At indicated times, 2×10^6 cells from a culture pulse labeled with [^{35}S]methionine (as described above) were incubated for 20 min at 0°C with an equal volume of ice-cold medium containing 20 mM potassium fluoride and 20 mM sodium azide. Cells were collected by centrifugation, suspended in 100 μl DB with 0.5% β-mercaptoethanol and incubated at 37°C for 30 min. One half of the sample was treated with protease, with addition of a one-quarter volume of 2,500 U/ml Pronase (in DB) for 60 min at 37°C. The other half was processed identically in parallel except that no protease was added. Protease was removed via two washes of the pelleted cells with 200 μl DB with 1 mM PMSF. Cells were then treated as described above for spheroplasting, extract preparation, and immune precipitation of STE3.

When Western analysis was used to assess susceptibility of receptor to external protease, the procedure was modified in several ways. For each timepoint, 3×10^8 cells were collected and prepared as above except that they were incubated in 0.5 ml DB with 0.5% β-mercaptoethanol at 37°C for 30 min before protease treatment. Proteolysis was terminated with the addition of TCA to 17%, samples were frozen on dry ice and then further processed as described (Ohashi et al., 1982), except that the TCA-extracted protein was precipitated for 10 min at 0°C, followed by a 10-min microfuge spin at 4°C. The pellet was washed once with acetone, dessicated, and dissolved at 70°C for 5 min in 100 μl SDS-PAGE sample buffer, 10 μl of which was then subjected to SDS-PAGE and immunoblotting.

As a control, accessibility of a cytoplasmic protein, phosphoglycerate kinase (PGK), was assessed with this protocol. No effects of protease treatment were observed. However, when Pronase was added subsequent to spheroplasting and treatment with 1% Triton X-100, PGK was found to be completely degraded.

Cell cultures were treated with a-factor by addition of an equal volume of cell-free filtrate prepared from a saturated culture of EG123 cells transformed with the a-factor overproduction plasmid pKK16 (Kuchler et al., 1989). Mock a-factor preparations were obtained from the isogenic *mfa1::LEU2 mfa2::URA3* strain SM1229.

Quantitation of Mating

To quantitate the mating efficiency of various *MAT*α strains after shut-off of receptor synthesis, 10^7 *MAT***a** cells (strain 227) were mixed either with 2×10^6 *MAT*α cells from a log phase YEPGalactose (2%) culture or with 2×10^6 cells from a YEPGalactose culture to which 3% glucose had been added during the final 2 h of growth. The mating mixtures were collected on nitrocellulose filters, and the filters were placed on YEPGalactose (2%) plates or on YEPGlucose (2%) plates. After 6 h at 30°C, the number of diploids was titered by suspending the cells and plating them on medium selective for diploids. Mating efficiency is expressed as the number of diploids divided by the total number of *MAT*α cells present on control filters that did not contain the *MAT***a** mate.

Isolation of ren Mutants

Cultures from 12 colonies of *mata1 GAL1–STE3* strain SY1498 carrying the *MAT*α plasmid pSL602 were treated with either 5.0, 1.5, 0.5% or no ethyl methane sulfonate for 1 h as described (Moir et al., 1982). Cells were then plated on 2% galactose minimal plates lacking uracil at a density of 3,000 viable cells per plate. Colonies were replica-plated to minimal glucose (2%) plates that had been spread with about 5×10^7 *MAT***a** cells (strain 227) in 0.3 ml of YEPD. Colonies that gave a strong mating reaction were picked for further study. Cells mutagenized with 1.5% ethyl methane sulfonate yielded mutants at a frequency of $\sim 10^{-3}$. On the other hand, no mutants were found in a screen of 20,000 unmutagenized cells.

From 10^5 colonies, 70 colonies that exhibited a strong mating reaction were picked. Of these, 45 mated when both growth and mating were done on glucose medium, a protocol that should preclude receptor synthesis. These were presumed to be defective for glucose repression of the *GAL* promoter and were therefore discarded. To determine whether the remaining mutants carried dominant or recessive mutations, they were crossed to *mata1* strain SY1498, and the mating phenotype of the resulting diploids was assessed by the same protocol used in the original mutant screen. 12 diploids showed strong mating and therefore the corresponding α mutants were presumed to carry dominant mutations. The other 13 mutants carried recessive mutations.

Indirect Immunofluorescence

Preparation of fixed, spheroplasted cells for indirect immunofluorescence was carried out essentially as described (Roberts et al., 1991), except that oxalyticase at a final concentration of 20 μg/ml was used for spheroplasting.

For detection of the receptor with the STE3 antiserum, antibodies that had been affinity-purified against the truncated fusion protein TrpE–STE3 Δ365 were used. These should react equally well with the STE3Δ365 receptor as they do with the wild-type protein. After incubation with the STE3 antibodies, used at a 1:20 dilution, signal was further amplified through three subsequent incubations with secondary antibodies (purchased from Jackson ImmunoResearch Laboratories Inc., West Grove, PA) used at 2 μg/ml: (*a*) goat anti-rabbit IgG; (*b*) rabbit anti-goat IgG; and (*c*) fluoresceinated goat anti-rabbit IgG. Antibody incubations were 1 h at room temperature.

For the double-staining of *myc*-tagged receptor and ALP, mouse mAb-1 (Oncogene Science Inc.) was used at a dilution of 1:20, while the rabbit anti-

Table I. Yeast Strains

Strain	Genotype	Reference
227	*MATalys1*	Herskowitz lab strain
EG123	*MATa ura3 leu2 trp1 can1 his4*	Siliciano and Tatchell, 1984
SM1229	isogenic to EG123, except *mfa1::LEU2 mfa2::URA3*	Michaelis and Herskowitz, 1988
YY1152	*MATα ste3::URA3 ura3 leu2 met14 ade2-1^{oc} ade1 his6 trp1^{am}*	Clark et al., 1988
SY1369	isogenic to YY1152, except Met$^+$	this work
SY1372	*MATα ste3Δ*	this work; A
SY1426	*MATα GAL1-STE3*	this work; A
SY1498	*mata1 GAL1-STE3*	this work; A
SY1534	*mata1 GAL1-STE3 ren1-1*	this work; A
SY1553	*MATa GAL1-STE3*	this work; A
SY1560	*MATα GAL1-STE3 ren1-1*	this work; A
SY1574	*MATα STE3*	this work; A
SY1579	*MATα STE3 ren1-1*	this work; A
SY1610	*MATα GAL1-STE3Δ365*	this work; A
SY1614	*MATa GAL1-STE3 ren1-1*	this work; A
SY1616	*MATα GAL1-STE3 pep4::URA3*	this work; A
SY1650	*MATα GAL1-STE3 ren1-1*	this work; A
SY1653	*MATα GAL1-STE3 ren1-1 pep4::URA3*	this work; A
SY1675	*MATa GAL1-STE3 pep4::URA3*	this work; A
SY1683	*MATα ste3Δ pep4Δ*	this work; A
SY1684	*MATα GAL1-STE3Δ365 pep4::URA3*	this work; A
SY1744	*MATα STE3 pep4::URA3*	this work; A
SY1960	*MATa STE3 GAL1-STE2*	this work; A
SY2029	*MATa STE3 GAL1-STE2 pep4::URA3*	this work; A
SY2041	*MATa STE3 GAL1-STE2 ren1-1*	this work; A
SY2559	*MATα GAL1-STE3Δ365(c-myc) pep4Δ*	this work; A
Sc252	*MATa ura3-52 leu2-3,112 ade1*	Whiteway et al., 1990
SY1793	isogenic to Sc252, except *MATα FUS1-HIS3 mfa1Δ mfa2Δ*	this work
SY1817	*MATα ste3Δ*	this work; B
SY1884	*MATα ste3Δ pep4Δ*	this work; B
SY2132	*MATα GAL1-STE3Δ365 pep4Δ*	this work; B
SY2152	*MATα GAL1-STE3 pep4Δ*	this work; B

Strains designated "A" in the reference column are isogenic to SY1369, except as indicated. Strains designated "B" are isogenic to SY1793.

ALP antiserum, which had previously been affinity purified and adsorbed against cells deleted for the ALP structural gene (*pho8Δ*), was used at 1:10. Detection of the *myc* antibody involved addition of 5 μg/ml biotinylated goat anti-mouse, followed by 5 μg/ml fluoresceinated streptavidin. Visualization of the anti-ALP antibodies was achieved via addition of 5 μg/ml rhodamine-conjugated goat anti-rabbit secondary antibodies.

Results

Rapid, Ligand-independent Endocytosis Delivers the a-factor Receptor to the Vacuole

As noted in the introduction, analysis of the abundance of

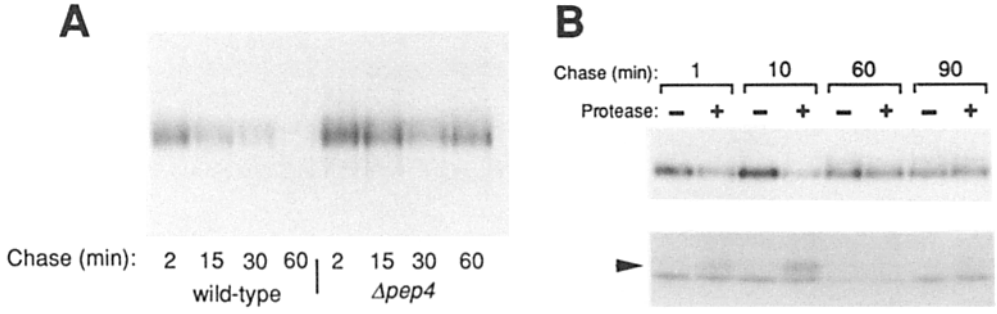

Figure 1. Turnover and surface accessibility of the a-factor receptor. (*A*) A wild-type *MATα* strain (SY1574) and its isogenic *pep4::URA3* derivative (SY1744) were labeled for 10 min with [^{35}S]methionine as described in Materials and Methods. Samples were taken 2, 15, 30, and 60 min after initiation of the chase, and then extracts were prepared and treated with STE3 antiserum. Immunoprecipitates were subjected to SDS-PAGE and STE3 was visualized by autoradiography. (*B*) *MATα pep4::URA3* cells (strain SY1744) were labeled for 10 min with [^{35}S]methionine. Samples were taken 1, 10, 60, and 90 min after initiation of the chase. Cells were digested with 1 mg/ml Pronase (+), or mock digested with no protease (−) for 1 h at 37°C. Extracts were prepared and treated as described above. The upper panel shows immune precipitated full-length STE3. The panel below shows an over-exposed portion of the same gel, with the arrow indicating the position of the 30-kD COOH-terminal STE3 digestion product.

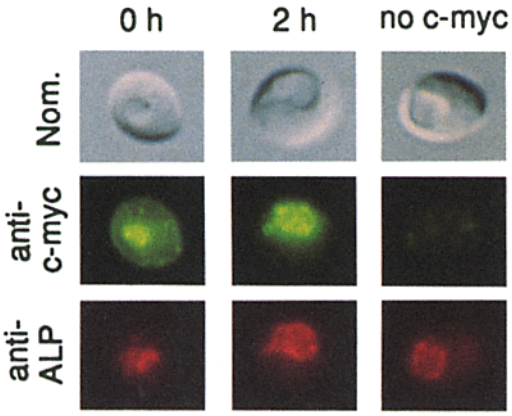

Figure 2. Indirect immunofluorescence of the c-*myc*–tagged receptor. *MATα pep4::URA3* cells (SY1616) cells carrying a *GALI-STE3-myc* construct (pSL2099) were grown for 4 h in the presence of 2% galactose, and 3% glucose was then added to repress further synthesis of the receptor. Samples to be prepared for microscopy were removed just prior to (*0 h*), and 2 h subsequent to the addition of glucose (*2 h*). Cells were fixed and prepared for immunofluorescence as described in the Materials and Methods. Fixed cells were treated with two antibody preparations, the anti-*myc* mAb-1 and affinity-purified polyclonal antiserum raised against the vacuolar membrane protein, ALP. As a control for background cross-reactivity of the anti-*myc* mAb, SY1653 cells transformed with the vector plasmid pRS315 were processed in parallel (*no c-myc*). The top panel shows a representative cell from each strain visualized by Nomarski microscopy. The middle panel shows the same cell stained with the anti-*myc* antibody. The bottom panel shows staining with antibodies to vacuolar alkaline phosphatase.

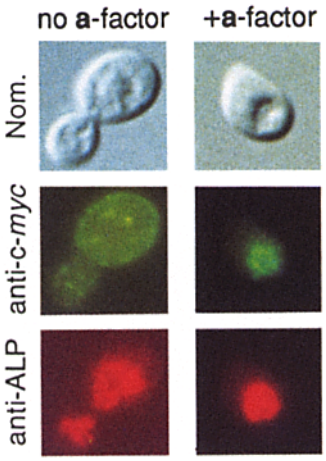

Figure 7. Immunofluorescent detection of the c-*myc*–tagged STE3 Δ365 receptor after treatment of cells with pheromone. *MATα GALI-STE3 Δ365(c-myc) pep4Δ* cells (SY2559) were grown for 4 h in the presence of 2% galactose, chased for 1.5 h with the addition of 3% glucose. Treatment with pheromone entailed the inclusion of a-factor during the glucose chase period. Cells were fixed and prepared for immunofluorescence as described in Materials and Methods. Fixed cells were treated with two antibody preparations, the anti-*myc* mAb-1 and affinity-purified polyclonal raised against the vacuolar membrane protein, ALP. The top panel shows a representative cell that has or has not been treated with a-factor visualized by Normarski microscopy. The middle panel shows the same cells stained with the anti-*myc* antibody. The bottom panel shows staining with the ALP-specific antibodies.

surface binding sites suggests that the yeast α-factor receptor is subject to ligand-mediated endocytosis (Jenness and Spatrick, 1986; Chvatchko et al., 1986). To analyze receptor fate directly in both the absence and presence of pheromone, we developed antibodies that recognize the COOH-terminal hydrophilic domain of the a-factor receptor, STE3 (Clark et al., 1988).

We first examined the stability of STE3 protein in the absence of added a-factor in wild-type cells, as well as in *pep4Δ* cells, which are deficient for vacuolar protease activity. STE3 protein was labeled with [^{35}S]methionine in a pulse–chase protocol, immunoprecipitated from cell extracts, and subjected to polyacrylamide gel electrophoresis. As shown in Fig. 1 *A*, STE3 was unstable in wild-type cells, exhibiting a half-life of ~20 min. In contrast, the receptor was extremely stable in the *pep4Δ* background, showing a half-life much greater than 2 h. Because of the possibility that a culture of α cells could contain low levels of a-factor (for instance, due to rare mating type switches) we also examined STE3 protein turnover in *MATα PEP4* cells deleted for the a-factor structural genes *MFA1* and *MFA2*. In these cells, the kinetics of STE3 turnover were identical to wild-type cells, indicating that turnover is indeed ligand independent (data not shown).

The rapid rate of receptor degradation and the dependence of this degradation on vacuolar proteases suggests that newly synthesized receptor is delivered to the cell surface, but resides there only a short time before being internalized and

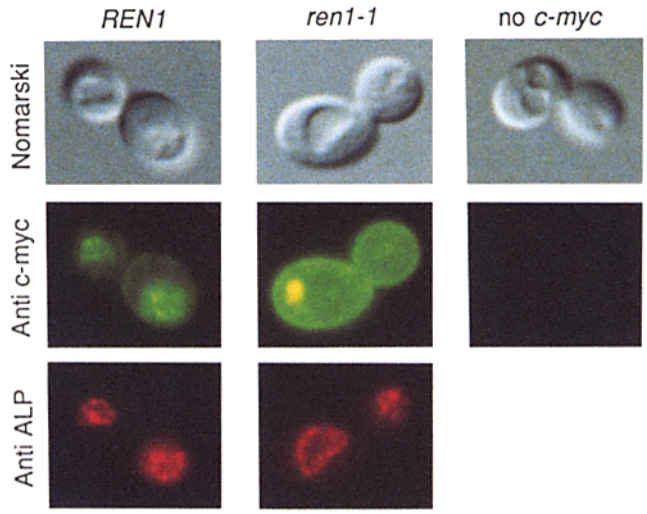

Figure 10. Indirect immunofluorescence of the c-*myc*–tagged receptor in *ren1* cells. *MATα pep4::URA3* cells (SY1616) or *MATα ren1 pep4::URA3* cells (SY1653) transformed with *GALI-STE3-myc* plasmid pSL2099 were grown for 4 h in the presence of 2% galactose, 3% glucose was added, and growth continued for an additional 30 min. Cells were fixed and prepared for immunofluorescence as described in Materials and Methods. Fixed cells were treated with two antibody preparations, the anti-myc mAb-1 and affinity-purified polyclonal antiserum raised against the vacuolar membrane protein, ALP. As a control for background cross-reactivity of the anti-*myc* mAb, SY1653 cells transformed with the vector plasmid pRS315 were processed in parallel (*no c-myc*). The top panel shows a representative cell from each strain visualized by Nomarski microscopy. The middle panel shows the same cell stained with the anti-*myc* antibody. The bottom panel shows staining with the ALP-specific antibodies.

delivered to the vacuole for degradation. As one test of this interpretation, we labeled receptor by a pulse–chase protocol and measured its susceptibility to digestion when whole cells were treated with exogenous protease (Trueheart and Fink, 1989). *pep4Δ* cells were used to preclude endogenous turnover of the receptor. As seen in Fig. 1 *B*, a small fraction of the STE3 protein, labeled during a 10-min [^{35}S]methionine pulse, was susceptible to protease after 1 min of chase. This susceptibility is revealed both by a reduction in the amount of full-length (48 kD) protein and by the appearance of a 30-kD digestion product. The mass of this product, coupled with its reactivity to the STE3 antiserum, implies that it corresponds to the seventh transmembrane segment and the COOH-terminal cytoplasmic domain. After 10 min of chase, ~70% of the radio-labeled receptor is susceptible to proteolysis by exogenous protease. We interpret these results to mean that only a small fraction of receptor synthesized during the 10-min pulse has been delivered to the cell surface by 1 min into the chase period but that the majority of the newly synthesized receptor is at the cell surface 10 min into the chase period. At longer chase times, the radio-labeled receptor is resistant to exogenous protease, suggesting that receptor that had been at the surface has been internalized (Fig. 1 *B*, 60- and 90-min timepoints). This internalization requires energy metabolism, as receptor remains susceptible to protease if potassium fluoride and sodium azide (10 mM each) are added 10 min into the chase period (data not shown).

As a second test of the idea that cell surface receptor is subject to constitutive internalization and delivery to the vacuole by an endocytic pathway, we determined the location of receptor by indirect immunofluorescence microscopy. For this analysis, STE3 was tagged at the COOH terminus with the c-*myc* 9E10 epitope (Evan et al., 1985), which is recognized by a mouse mAb. The tagged receptor complemented *ste3* mutations, and like wild-type STE3, showed rapid turnover (data not shown). To facilitate detection of the receptor-derived immunofluorescence signal, the c-*myc*–tagged *STE3* was placed under the control of the inducible *GAL1* promoter. Expression from the *GAL1* promoter results in a 10–20-fold over-production of the STE3 protein (data not shown), but this over-production caused no change either in the receptor's sorting to the surface or its subsequent internalization. In particular, as shown below, STE3 protein expressed from the *GAL1* promoter showed rapid *PEP4*-dependent turnover (see Fig. 3). Moreover, the kinetics of receptor delivery to the surface and subsequent internalization as measured by protease susceptibility in *GAL1–STE3 pep4Δ* cells paralleled the kinetics shown in Fig. 1 *B* (data not shown).

We examined the receptor's location both under conditions of continuous synthesis and 2 h subsequent to a glucose-mediated repression of new receptor synthesis (Fig. 2). The cells are *pep4Δ* so that receptor degradation is blocked. Under conditions of ongoing receptor synthesis, the receptor was found to locate to two distinct places—the cell surface and an internal compartment. This internal compartment is inferred to be the vacuole because the same compartment is stained by antibodies to the vacuolar membrane protein, ALP. Moreover, receptor staining overlays the vacuole, as defined by depressions seen by Nomarski microscopy (Fig. 2). 2 h subsequent to the shut-off of new receptor synthesis, no surface staining was evident. Rather, essentially all of the receptor-derived fluorescence signal was seen to overlay the vacuole. Loss of surface fluorescence likely reflects the internalization of surface receptor and its delivery to the vacuole.

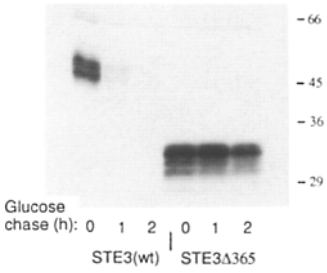

Figure 3. Turnover of the COOH-terminal Truncated Receptor. *MATα ste3Δ* cells (SY1817) carrying *GAL1–STE3* (pSL552) or *GAL1–STE3Δ365* (pSL1922) were grown to log phase on galactose medium. Receptor synthesis was shut off with the addition of 3% glucose. Samples were taken just before glucose addition and at 1 and 2 h after glucose addition. STE3 was visualized by Western analysis of extracts. Molecular weight standards (in kilodaltons) are indicated at right.

As a further test of the conclusion that the a-factor receptor is routed to the vacuole via endocytosis from the cell surface, we examined the effect of the *sec1^{ts}* mutation on receptor location. At the restrictive temperature, delivery of newly synthesized proteins to the surface is blocked in *sec1^{ts}* cells; surface-targeted proteins instead accumulate in secretory vesicles (Novick and Schekman, 1979). In contrast, delivery of proteins whose primary destination is the vacuole proceeds normally in *sec1* cells (Stevens et al., 1982; Roberts et al., 1989). After temperature shift of *MATα pep4Δ sec1^{ts}* cells, expression of a *GAL1*-driven c-*myc*–tagged STE3 protein was induced with galactose and receptor visualized by immunofluorescence. No vacuolar staining was seen (data not shown). Instead dispersed punctate cytoplasmic staining was found often concentrated near the growing end of the cell (data not shown). Thus, delivery of receptor to the vacuole requires prior delivery to the cell surface.

Receptor COOH-terminal Truncation Mutants Are Disabled for Constitutive Endocytosis

Mammalian cell surface receptors that undergo constitutive,

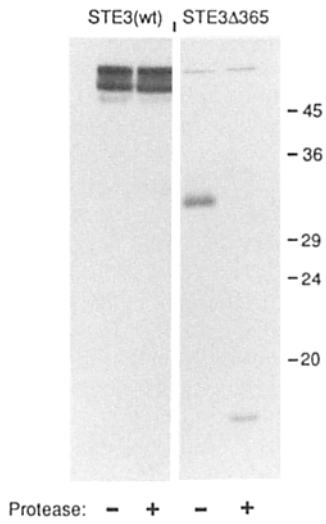

Figure 4. Susceptibility of the COOH-terminal truncated receptor to exogenous protease. *MATα pep4::URA3* cells that were *GAL1–STE3* (SY1616) or *GAL1–STE3Δ365* (SY1684) were grown for 2.5 h in the presence of 2% galactose, 3% glucose was added, and growth continued for 2.5 h. Whole cells were digested with 1 mg/ml Pronase (+), or mock digested with no protease (−) for 1 h at 37°C. Subsequently, extracts were prepared and subjected to Western analysis using STE3 antiserum. Molecular weight standards (in kilodaltons) are indicated at right.

ligand-independent endocytosis have been found to have sequences in their cytoplasmic domains that direct sequestration into clathrin coated pits and subsequent internalization (Trowbridge, 1991). Receptor mutants deleted for these "endocytosis signals" do not get internalized. To examine the role of STE3 protein's 187-residue COOH-terminal cytoplasmic domain in receptor endocytosis, we constructed *STE3* mutants partially truncated for this domain. These mutants retain the ability to function in signal transduction as they fully complemented *ste3Δ* alleles. The receptor structural genes were placed under control of the inducible *GAL1* promoter and the ability of the mutant receptors to be internalized was evaluated by the same assays used above for wild-type receptor: *PEP4*-dependent turnover, accessibility to surface protease, and indirect immunofluorescence.

To follow turnover, cells with either wild-type or mutant receptor *GAL1* constructs were grown on galactose, to allow expression, and then glucose was added to block further synthesis. At intervals, samples were withdrawn and STE3 abundance was assessed by Western analysis of cell extracts. As with the radioactive pulse-chase experiment, wild-type STE3 was rapidly turned over (Fig. 3). STE3Δ433, missing the COOH-terminal 37 residues, showed a stability similar to wild-type receptor (data not shown). In contrast, STE3Δ399 and STE3Δ365, missing 71 and 105 residues, were very stable and showed no degradation two hours after the block to new synthesis (Fig. 3 and data not shown). The degradation of STE3 protein therefore requires a segment of the COOH-terminal domain.

Accessibility of receptor to exogenous protease was assessed in *pep4Δ* cells having either the *GAL1–STE3* or the *GAL1–STE3Δ365* construct. Cells were grown in galactose for 2.5 h, glucose was added to halt further synthesis, and protease treatment was initiated after a 2.5-h incubation in the glucose medium. As seen previously with radiolabeled STE3 (Fig. 1 *B*), wild-type receptor accumulated in a protease-resistant compartment (Fig. 4), presumably the vacuole. The protease susceptibility of STE3Δ365 protein was markedly different from wild-type STE3. Even 2.5 h after imposition of the glucose block to synthesis all truncated receptor was sensitive to external protease, as revealed by the disappearance of the 33-kD STE3Δ365 band and the appearance of the 18-kD digestion product.

Finally, by indirect immunofluorescence microscopy, the STE3Δ365 protein accumulated at the cell surface (Fig. 5), whereas wild-type receptor accumulated in the vacuole, as before (Fig. 2). The surface accumulation of STE3Δ365 does not result from its overproduction from the *GAL1* promoter. When expressed from its natural promoter, STE3-Δ365 was stable and exclusively located at the cell surface (data not shown). We conclude that the STE3Δ365 receptor is not subject to constitutive endocytosis.

Ligand-dependent Receptor Internalization

The experiments described thus far establish that the a-factor receptor is internalized continuously in the absence of ligand. Does the receptor also exhibit ligand-induced endocytosis? To answer this question we took advantage of STE3Δ365, which is disabled for constitutive endocytosis. Synthesis of receptor was induced by growth of *GAL1–STE3Δ365 pep4Δ* cells in galactose for 90 min and receptor was allowed to accumulate at the cell surface during a 60-min glucose chase. The location of the receptor was evaluated by the extracellular protease assay at various times after addition of a-factor. In the absence of added a-factor, STE3Δ365 was susceptible to digestion by external protease (Fig. 6). In this experiment the cytoplasmic domain digestion product was run off the gel, so protease susceptibility is manifest only by the disappearance of the receptor protein. 10 min after a-factor addition, a substantial portion of the receptor was resistant to protease, and after 90 min, the receptor protein was completely resistant to protease. We conclude that pheromone caused the receptor to be removed from the surface and delivered to an internal cellular compartment. Thus, although STE3Δ365 is totally disabled for constitutive endocytosis, it remains capable of a pheromone-dependent internalization.

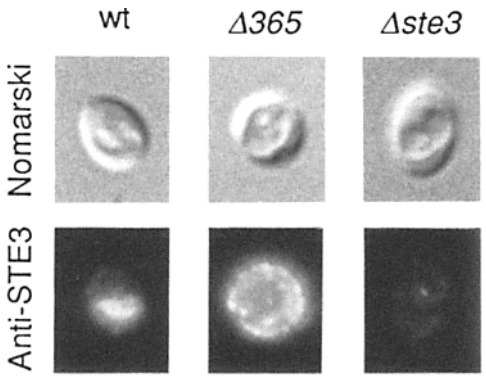

Figure 5. Indirect immunofluorescence of the COOH-terminal truncated receptor. *MATα pep4Δ* cells harboring either *ste3Δ* (SY1884), *GAL1–STE3* (SY2152), or *GAL1–STE3Δ365* (SY2132) at the chromosomal *STE3* locus were grown for 5 h in the presence of 2% galactose, 3% glucose was added, and growth was continued for an additional hour. Cells were fixed and prepared for immunofluorescence as described in Materials and Methods. The top panel shows a representative cell of each strain visualized by Nomarski microscopy. Cell surface depressions correspond to vacuoles. The panels below show the same cells under fluorescent conditions, stained with STE3 antiserum.

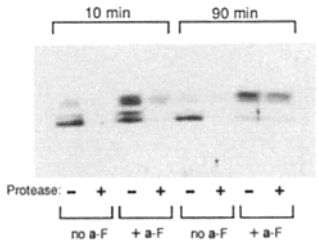

Figure 6. Susceptibility of the COOH-terminal truncated receptor to exogenous protease after treatment of cells with pheromone. *MATα GAL1–STE3 Δ365 pep4Δ* cells (SY2132) were grown for 1.5 h in the presence of 2% galactose, chased for 1 h with 3% glucose, and then treated with pheromone or mock pheromone. At the times indicated, samples were removed and 10 mM sodium azide was added. Whole cells were then subjected to surface proteolysis with 1 mg/ml Pronase (+) for 1 h at 37°C or mock digested (−) with no protease. STE3Δ365 protein was visualized by Western analysis.

Correlated with the change in subcellular location, pheromone also caused extensive covalent modification of the receptor protein, as seen in Fig. 6. Although we have not investigated the nature of this modification, it is known that other members of this receptor family, including the α-factor receptor, show increased phosphorylation on the COOH-terminal domain in response to hormone (Reneke et al., 1986; Dohlman et al., 1991).

a-factor–dependent internalization was also followed by indirect immunofluorescence microscopy. For this experiment, the STE3Δ365 receptor was tagged at its COOH terminus with the c-*myc* 9E10 epitope (Evan et al., 1985) and placed under the control of the *GAL1* promoter. These cells were cultured via the galactose–glucose protocol and then treated with a-factor or mock pheromone for 1.5 h. The mock-treated cells primarily showed surface staining (Fig. 7). In contrast, after a-factor treatment no surface staining was evident. Instead all of the receptor-derived fluorescence signal was seen to be vacuolar, showing complete coincidence with the ALP-derived fluorescence and with the vacuolar depressions seen by Nomarski microscopy (Fig. 7).

Constitutive and Ligand-dependent Endocytosis Are both G Protein-independent Processes

The endocytic uptake of α-factor pheromone and the correlated loss of surface binding sites was found to proceed upon pheromone challenge in *MAT***a** cells lacking the heterotrimeric G protein (Jenness and Spatrick, 1986; Zanolari et al., 1992). To determine whether the constitutive or ligand-mediated endocytosis of the a-factor receptor requires the G protein, we expressed *GAL1–STE3* or *GAL1–STE3Δ365* receptor constructs in diploid cells, which do not transcribe the G protein structural genes (Miyajima et al., 1987; Dietzel and Kurjan, 1987; Whiteway et al., 1989). Both constitutive and ligand-dependent endocytosis proceeded with normal kinetics (data not shown). This implies that the endocytic machinery recognizes the receptor proper, not a G protein/receptor complex.

Genetic Screen for Trans-acting Mutants that Block Endocytic Turnover of STE3 Protein

The different locations of wild-type STE3 and STE3Δ365 proteins following the galactose to glucose pulse–chase protocol might result in different mating capacities for strains carrying these constructs. We therefore compared the ability of *GAL1–STE3* and *GAL1–STE3Δ365* strains to mate under several conditions. When growth and mating were carried out on galactose medium, which allows continuous receptor synthesis, the strains mated equally well (Table II). However, when cells were grown on galactose but transferred to glucose medium 2 h before mating, *GAL1–STE3Δ365* cells mated efficiently, but *GAL1–STE3* cells mated poorly (Table II). The ability of the *STE3Δ365* cells to mate appears to reflect the retention of receptor at the surface rather than simply the failure to degrade the receptor, as *GAL1–STE3 pep4Δ* cells mated poorly even though the receptor is stable (Table I).

We took advantage of the mating difference of *GAL1–STE3* and *GAL1–STE3Δ365* to isolate mutants disabled for receptor internalization. Mutagenized *GAL1–STE3* cells were screened for mutants that showed strong mating following glucose-mediated repression of new receptor synthesis, and 25 mutant colonies were identified (see Materials and Methods). To determine whether the mutations were dominant or recessive, the mutants were mated to a *matal* strain and the mating properties of the resulting α/al⁻ diploid assessed in the galactose/glucose protocol (note: α/al⁻ diploids mate as α cells; Kassir and Simchen, 1976). By this criterion 12 of the 25 mutants carried dominant mutations. Of these, four are likely chain termination mutations in *STE3* because immunoblotting revealed that they expressed truncated forms of STE3 protein. The other eight dominant mutations may be *STE3* alleles that lead to more subtle alterations in STE3 or they may be mutant alleles of other genes.

Analysis of ren1-1 Mutants

The recessive mutations should identify *trans*-acting functions required for endocytosis. We chose a particularly strong example of this class for further study. This mutation segregated as a single gene unlinked to *STE3*. As the mutant is defective in receptor endocytosis (see below), the gene has been named *REN1*. We quantitated the mating of *ren1-1* cells in the galactose–glucose mating protocol used to isolate the mutant. As shown in Table II, *ren1-1* cells mated as well as *GAL1–STE3Δ365* cells. Northern blot analysis showed that *ren1-1* does not affect the synthesis or stability of *STE3* mRNA. Moreover, glucose repression of *GAL1–STE3* mRNA synthesis occurred with identical kinetics in wild-type and *ren1-1* cells (data not shown). We therefore considered it likely that *ren1-1* affected receptor endocytosis and tested the possibility directly.

Table II. Mating Capacity of Mutants Defective for Endocytosis or Turnover of STE3 Protein

Strain	Relevant genotype	Efficiency of mating	
		Gal-to-Gal	Gal-to-Glu
SY1426	*GAL1–STE3*	0.9	0.0003
SY1610	*GAL1–STE3Δ365*	0.8	0.3
SY1616	*GAL1–STE3 pep4::URA3*	0.9	0.001
SY1650	*GAL1–STE3 ren1-1*	0.9	0.3

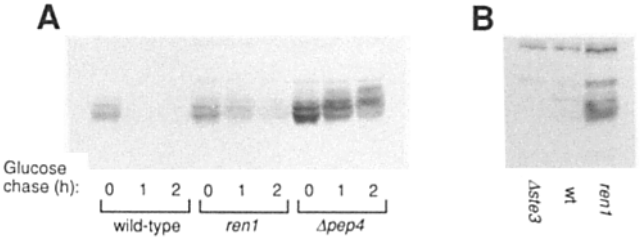

Figure 8. Turnover of the a-factor receptor in *ren1* cells. (*A*) Wild-type *MATα GAL1–STE3* cells (SY1426), *ren1-1* mutants (SY1650), and *pep4::URA3* mutants (SY1616) were grown for 3 h in the presence of 2% galactose, 3% glucose was added, and incubation was continued for several hours. Protein extracts were prepared from samples taken just before glucose addition and at 1 and 2 h after addition. STE3 was visualized by Western analysis. (*B*) To assess the steady state level of STE3 protein, extracts were prepared from exponential cultures of *MATα ste3Δ* cells (SY1372), wild-type *MATα* cells (SY1574), and *MATα ren1-1* cells (SY1579). STE3 was visualized by Western analysis.

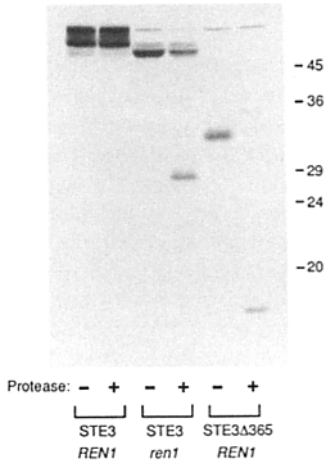

Figure 9. Susceptibility of the receptor in *ren1* cells to exogenous protease. The location of the receptor in three *pep4::URA3* strains was assessed using surface proteolysis. *MATα GAL1–STE3* (SY1616), *MATα GAL1–STE3 ren1-1* (SY1653), and *MATα GAL1–STE3Δ365* (SY1684) cells were grown and treated as described in the legend to Fig. 3. An immunoblot of the resulting cell extracts is shown, using STE3 antiserum as probe. Note that the electrophoretic mobility of STE3 protein from REN1$^+$ cells is slowed relative to its mobility when extracted from *ren1-1* cells. This mobility shift is most readily observed in *pep4* cells and we therefore believe that it reflects a modification that occurs in the vacuole where the receptor accumulates. Molecular weight standards (in kilodaltons) are indicated at right.

ren1-1 Slows STE3 Turnover

We examined the turnover of wild-type STE3 protein in both *REN1*$^+$ and *ren1-1* cells using the galactose–glucose pulse-chase protocol. In wild-type cells, receptor turnover was rapid. In *ren1-1* cells, however, turnover was slowed considerably (Fig. 8 *A*). In separate pulse-chase experiments with [^{35}S]methionine, STE3 expressed from its own promoter exhibited a half-life of ~90 min in the *ren1-1* background (data not shown), compared to 20 min in *REN1*$^+$ cells (Fig. 1). Mutations that slow STE3 protein turnover should lead to steady state over-accumulation of the receptor. In keeping with this expectation, STE3 protein expressed from its natural promoter was found to be more abundant in *ren1-1* cells than in wild-type cells (Fig. 8 *B*).

The experiments described above established that constitutive turnover of wild-type STE3 is slowed in *ren1-1* mutants. Ligand-mediated turnover of STE3Δ365 was also slowed in *ren1-1* cells (data not shown).

STE3 Protein of ren1-1 Cells Is Susceptible To Extracellular Protease

The mating and receptor turnover phenotypes of the *ren1-1* mutant are very similar to those of cells expressing STE3Δ365 protein. We were therefore interested to compare the location of STE3 protein in *ren1-1* cells to its location in wild-type cells. We first used the extracellular protease assay and the *GAL1* constructs to evaluate receptor location after a galactose to glucose pulse-chase protocol. As expected, protease caused essentially no diminution of the full-length wild-type STE3 protein expressed in wild-type cells, and only a small amount of released cytoplasmic tail digestion product was observed (Fig. 9). Under the same conditions, all of the STE3Δ365 protein was susceptible to the protease and was converted to its corresponding cytoplasmic domain digestion product. The result for *ren1-1* cells is intermediate between these two extremes. In the *ren1-1* background, STE3 protein was partially susceptible to the external protease, and a substantial amount of the cytoplasmic tail digestion product was seen (Fig. 9). However, in contrast to the results seen for STE3Δ365, a substantial fraction of total STE3 protein was resistant to protease.

Internalized STE3 Is Extra-vacuolar in ren1-1 Cells

The experiments described above imply that constitutive endocytosis may be impaired, but not completely blocked, in the *ren1-1* background; some receptor clearly is internalized by the mutant cells. To determine the location of this internalized receptor we stained mutant and wild-type cells with antibodies that recognize the *myc*-tagged STE3 protein and antibodies that recognize the vacuolar membrane protein, ALP. 30 min after glucose-mediated shut off of the *myc*-tagged *GAL1–STE3 ren1-1*, but not *REN1*$^+$ cells, retained a significant amount of receptor at the cell surface (Fig. 10). Both genotypes also exhibited internal staining for receptor, but the pattern of staining was markedly different. In the *REN1*$^+$ background, internalized receptor was vacuolar. Receptor staining showed complete colocalization with the immunofluorescent signal from the vacuolar marker protein ALP. Furthermore both signals coincided with vacuolar depressions seen by Nomarski microscopy. Most *ren1-1* cells, on the other hand, showed little or no overlap of the two signals. Instead, bodies staining brightly for the receptor were often seen adjacent to the vacuole. Such bodies may represent an intermediate endocytic compartment through which the receptor normally passes on its way from surface to vacuole.

Similar extra-vacuolar bodies have recently been described for a subset of mutants defective in vacuolar protein sorting, Class E *vps* mutants (Raymond et al., 1992). *vps* mutants were selected for their aberrant secretion to the culture medium of the soluble vacuolar protease, carboxypeptidase Y (CPY) (Bankaitis et al., 1986; Rothman and Stevens, 1986). The Class E mutant subset secretes ~40% of newly synthesized CPY. In addition, CPY that remains intracellular occupies a novel compartment. By immunofluorescence microscopy, it is found to stain bodies located just adjacent to the vacuole. These structures also contain several other vacuolar membrane proteins whose vacuolar delivery is also presumably blocked (Raymond et al., 1992).

Because of this morphological similarity of *ren1* cells with Class E *vps* mutants, we asked if *ren1* showed a *vps* sorting defect for CPY. Indeed, like the Class E *vps* mutants, *ren1-1* cells were shown to secrete some CPY (data not shown).

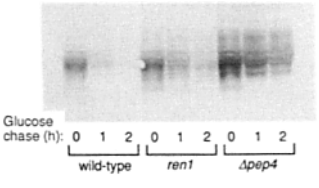

Figure 11. Turnover of the α-factor receptor. Wild-type *MATa* (SY1960), *ren1-1* (SY2041), and *pep4::URA3* (SY2029) cells that carry *GAL1–STE2* at the *STE2* locus were grown for 3 h in the presence of 2% galactose, 3% glucose was added, and growth continued for several hours. Protein extracts were prepared from samples taken just before glucose addition, and at 1 and 2 h after glucose addition. STE2 was visualized by Western analysis using antisera generously provided by James Konopka.

Given that *ren1-1* cells exhibit a weak *vps*⁻ phenotype, we considered the possibility that *ren1-1* may be an allele of a known *VPS* gene. Complementation analysis of *ren1-1* with the complete set of *vps* mutants indicated an identity with *vps2*, a member of the Class E subset (Raymond et al., 1992).

Turnover of the α-factor Receptor Is REN1- and PEP4-dependent

To extend the analysis of receptor turnover, we examined the metabolism of the other pheromone receptor, the α-factor receptor (STE2), in a variety of genetic backgrounds using a *GAL1-STE2* construct. Like STE3 protein, STE2 protein was degraded rapidly in wild-type cells during the glucose chase. The *ren1-1* mutation slowed this turnover, and *pep4Δ* blocked turnover altogether (Fig. 11).

Discussion

Pheromone Receptors Are Subject to Two Modes of Endocytosis

Two distinct modes of endocytosis appear to operate on the yeast a-factor receptor: a constitutive, ligand-independent mechanism and a regulated, ligand-dependent mechanism. In both types of endocytosis the receptor traverses the same subcellular territory, moving from the cell surface to the vacuole where it is degraded.

Three experimental observations established that the a-factor receptor is subject to endocytosis in the absence of ligand. First, pulse-chase experiments demonstrate that the receptor is an unstable protein whose degradation depends on vacuolar proteases. Second, using exogenous protease to measure the amount of receptor present at the cell surface, we found that newly synthesized a-factor receptor remains protease sensitive only for a short interval after its delivery to the surface, implying a rapid constitutive internalization. Finally, indirect immunofluorescence assays show that over the same time course the receptor accumulates in the vacuole. Together our results provide the following picture of the dynamics of receptor trafficking. Newly synthesized receptor is delivered via the secretory pathway to the cell surface where it resides only transiently, exhibiting a half-life of ~20 min. Receptor is then internalized and delivered to the vacuole where it is degraded.

A second mode of endocytosis was recognized because of the properties of a-factor receptor mutants lacking half of the COOH-terminal cytoplasmic domain. These mutants fail to undergo constitutive endocytosis, suggesting that the *STE3 Δ365* and *STE3Δ399* mutations delete "signals" on the receptor necessary to this process. For example, perhaps these signals are required for capture into clathrin-coated pits (see below). Despite the block to constitutive endocytosis, these mutant receptors are still subject to ligand-mediated endocytosis. Because the mutant receptors are defective for one mode of endocytosis but not the other, we suggest that there is at least one mechanistic step that distinguishes the two classes of endocytosis. Another possibility is that the endocytosis machinery recognizes a holistic feature of the COOH-terminal cytoplasmic domain, perhaps the extent of a posttranslational modification. In this view, the COOH-terminal receptor mutants after pheromone treatment would show the same extent of modification as wild-type receptor exhibits in the absence of pheromone.

The α-factor receptor also exhibits both modes of endocytosis. By assays identical to those used to analyze the a-factor receptor, we showed that the α-factor receptor is subject to rapid constitutive endocytosis. Previous studies implied that the α-factor receptor was also subject to ligand-mediated endocytosis. In particular, it was found that when cells were treated with pheromone, cell surface binding sites were lost rapidly (half-life ~20 min) (Jenness and Spatrick, 1986; Konopka et al., 1988; Reneke et al., 1988), presumably reflecting endocytosis of the receptor. Although not the focus of these studies, the experiments also provided hints that the α-factor receptor undergoes constitutive endocytosis. In particular, a slow loss of α-factor binding sites was observed in the absence of ligand (surface half-life >2 h at 25°C; about 45 min at 34°C). This rate differs considerably from the rapid turnover we observe for both pheromone receptors and likely reflects the different protocol used (their experiments were carried out in the presence of cycloheximide at 25 or 34°C). Nonetheless, it seems likely that the two experimental protocols reveal the same process, as α-factor receptors deleted for part of the COOH-terminal cytoplasmic domain were blocked for this slow constitutive loss of binding sites, but remained competent for the ligand-mediated loss (Konopka et al., 1988). If this interpretation is correct, these data again imply that constitutive and ligand-mediated endocytosis may have a different mechanistic basis.

The rapid constitutive endocytosis of the pheromone receptors is not likely due to bulk endocytosis of the plasma membrane. Rather, two observations imply that the capacity for constitutive endocytosis is specifically built in to these proteins. First, the COOH-terminally truncated receptors, STE3Δ365 and STE3Δ399 fail to undergo constitutive endocytosis presumably because they lack requisite signals. Second, the plasma membrane ATPase is turned over very slowly, showing a half-life of >10 h (Benito et al., 1991).

Possible Roles for Constitutive Endocytosis

Constitutive endocytosis of the pheromone receptors seems at first glance to be an unproductive and unnecessary process. What purpose might it serve? Two possibilities are especially appealing. First, receptor endocytosis may facilitate the switch in receptor type that must occur when yeast cells undergo mating-type interconversion. Most wild strains of yeast are homothallic and under certain conditions can change mating types as frequently as every cell division cycle. The change is effected by a switch in the genetic information present at the mating-type locus, which then directs the synthesis of the receptor and pheromone species appropriate for the new mating type. This rapid phenotypic conversion of mating type likely requires removal of old receptor because cells that express both receptors are defective for mating (Bender and Sprague, 1989). Constitutive endocytosis provides a rapid means to achieve removal of old receptor.

A second role for constitutive endocytosis may be in partner selection during the mating process. a and α cells sense the location of nearby potential mating partners, apparently by detecting a gradient of pheromone concentration (Jackson and Hartwell, 1990*a*,*b*). In response, they reorient cell

polarity and focus growth toward the partner. Newly synthesized receptor is therefore deposited at the region of the cell surface nearest the partner. The simultaneous removal of receptor from other surface sites by constitutive endocytosis would reinforce the emerging asymmetric receptor distribution. Thus, constitutive endocytosis may be an important component of partner selection during the courtship phase of mating. In keeping with this possibility, strains expressing COOH-terminal truncated receptors are impaired for partner selection (Jackson and Hartwell, 1990*a*; C. Boone, N. Davis, and G. Sprague, unpublished results).

In principle, constitutive endocytosis could also serve as a means to set the cell's level of sensitivity to pheromone. COOH-terminal truncated receptors are defective for constitutive endocytosis and also confer increased sensitivity to pheromone (Konopka et al., 1988; Reneke et al., 1988; C. Boone, N. Davis and G. Sprague, unpublished results). However, we infer that the correspondence of these two receptor properties is fortuitous because *renl* mutants, which are impaired for constitutive endocytosis of wild-type receptor, do not show increased sensitivity to pheromone (N. Davis and G. Sprague, unpublished results). Thus, it seems unlikely that constitutive endocytosis plays a major role in determining sensitivity to pheromone.

Functions Required for Endocytosis

To begin to identify gene products required for endocytosis we developed a screen to isolate mutants defective for the process. The screen uses a simple mating assay to reveal mutants that retain functional receptor at the surface after a shut off of new receptor synthesis. In principle, mutants may be blocked either at the initial stages of endocytosis or at any stage from which endocytic vesicles can recycle to the surface. In this context, it should be noted that receptors located in the vacuole cannot be recycled to the surface. This conclusion follows from the observation that *pep4* mutants, which accumulate receptor in the vacuole, cannot mate in the assay (Table II). Thus, the mutant isolation scheme will not reveal functions that are simply required for vacuolar proteolytic activity. The scheme requires that the mutants be defective for constitutive endocytosis, but they may also be defective for ligand-mediated endocytosis if the two processes share common steps.

Analysis of one mutant strain revealed that constitutive endocytosis is indeed altered. In this *renl* strain, receptor accumulates in two locations—at the cell surface and in an intracellular compartment that lies near the vacuole. We suggest that this compartment represents a yeast endosome. The *renl* defect apparently blocks traffic from the putative endosome to the vacuole. In animal cells, the endosome serves a crossroads where the fate of internalized material is decided—whether to continue on to the lysosome for degradation or to exit the pathway, as many receptors do, and recycle back to the cell surface. If recycling occurs in yeast, then the accumulation of receptor at the surface of *renl* mutant cells could be a secondary result of a *renl*-imposed block to vacuolar delivery. Receptor that accumulates in the endosome may be free to recycle back to the surface via an existing recycling pathway. Alternatively, the accumulation of receptor at the surface may indicate that *REN1* has a direct role in receptor internalization. Although our analysis of the *renl-1* mutant has focused on constitutive endocytosis, the observation that ligand mediated turnover of receptor (STE3Δ365) is slowed in *renl-1* cells indicates that REN1 is also required for ligand mediated endocytosis.

The finding that *REN1* is identical to *VPS2* implies that this gene is required for proper function of two modes of transport to the vacuole—transport of proteins internalized by endocytosis and the transport of newly synthesized vacuolar enzymes. One possibility is that these two pathways converge at a point before delivery to the vacuole and that *REN1/VPS2* is required to carry out a step after the convergence. Indeed, in animal cells, a similar convergence of lysosome biogenic and endocytic pathways has been established (Griffiths et al., 1988). In keeping with this possibility, Class E *vps* mutants, including *vps2*, accumulate a novel organelle that contains a number of newly synthesized proteins normally destined for vacuolar delivery: CPY, the vacuolar ATPase, and diamino-dipeptidyl peptidase B (Raymond et al., 1992). (We note, however, that not all vacuolar proteins—in particular ALP—are impaired for delivery to the vacuole; for discussion see Raymond et al., 1992.) These organelles are likely identical to those containing internalized a-factor receptor that we observe in the *renl* mutants. Proof of this will await double-stained immunofluorescence showing colocalization of endocytosed receptor and vacuolar proteins within these presumptive endosomes.

Although not identified by our small collection of Ren$^-$ mutants, clathrin appears to be a second function required for constitutive endocytosis. As noted in the introduction, disruption of the clathrin heavy chain gene leads to a reduction in the rate of α-factor uptake (Payne et al., 1988). Moreover, we find that a temperature-sensitive mutation in this gene leads to a reduction both in the rate of α-factor uptake and in the constitutive internalization of the a-factor receptor upon shift to nonpermissive temperature (P. Tan, N. Davis, G. Sprague, and G. Payne, unpublished results). The rapid onset of these phenotypes after temperature shift implies a direct role for clathrin in the endocytosis of the yeast pheromone receptors.

Recently, three newly identified genes have been suggested to have a role in the endocytosis of the yeast pheromone receptors (Wichmann et al., 1992; Raths et al., 1993). Mutation of these genes results in a defect in the uptake and/or degradation of the α-factor pheromone. *end3* and *end4* mutant cells display surface binding sites for α-factor pheromone but are defective for pheromone uptake, implying that they are defective for the initial step of receptor internalization from the surface (Raths et al., 1993). On the other hand, the yeast *YPT7* gene, isolated by virtue of homology to *Rab7*, which encodes a late endosome-associated GTP-binding protein in animal cells, may control a later step in the endocytic pathway. Disruption of *YPT7* blocks α-factor degradation, but not the initial uptake of pheromone by the mutant cells (Wichmann et al., 1992). However, the defect in α-factor degradation associated with *ypt7* mutants may not be due to impaired endocytic transport. Instead, it may reflect impaired vacuolar function. Indeed, *ypt7* mutant cells show a generalized defect in the processing of vacuolar zymogens as well as a grossly disrupted vacuolar morphology (Wichmann et al., 1992).

Our analysis of the endocytosis of the yeast pheromone receptors has begun to define discrete steps in a pathway for receptor transport connecting the cell surface to the vacuole.

The finding that the endocytic and vacuolar biogenic pathways likely converge in yeast, just as they do in animal cells, coupled with the involvement of clathrin and the possible involvement of Rab proteins in both the yeast and animal cell processes (Chavrier et al., 1990; van der Slijs et al., 1991, 1992; Bucci et al., 1992; Wichmann et al., 1992), implies that many functions required for endocytosis in yeast will have animal cell counterparts. Analysis of additional Ren$^-$ mutants should identify such functions.

We thank Chris Raymond, James Konopka, and Karl Kuchler for generously providing antisera and plasmids. We thank Charlie Boone, David Hagen, Chris Raymond, and Tom Stevens for comments on the manuscript as well as for helpful discussions throughout the course of this work. We also thank Lynne Chase for help in preparing this manuscript. Special thanks to Isabelle Howald-Stevenson for the complementation analysis demonstrating the identity of *ren1* with *vps2*.

This work was supported by research grants from the U.S.P.H.S. (GM 38157 and GM 30027) and by a Faculty Research Award from the American Cancer Society (FRA-282). N. Davis was supported by fellowships from U.S. Public Health Service (U.S.P.H.S.) (GM1 12672) and from the Oregon Affiliate of the American Heart Association. J. Horecka was supported by a training grant from U.S.P.H.S. (GM 07759).

Received for publication 22 March 1993 and in revised form 15 April 1993.

References

Anderson, R. G. W., E. Vasile, R. J. Mello, M. S. Brown, and J. L. Goldstein. 1978. Immunocytochemical visualization of coated pits and vesicles in human fibroblasts: relation to low density lipoprotein receptor distribution. *Cell.* 15:919–933.

Bankaitis, V. A., L. M. Johnson, and S. D. Emr. 1986. Isolation of yeast mutants defective in protein sorting to the vacuole. *Proc. Natl. Acad. Sci. USA.* 83:9075–9079.

Basu, S. K., J. L. Goldstein, R. G. W. Anderson, and M. S. Brown. 1981. Monensin interrupts the recycling of low density lipoprotein receptors in human fibroblasts. *Cell.* 24:493–502.

Bender, A., and G. F. Sprague, Jr. 1986. Yeast peptide pheromones, a-factor and α-factor, activate a common response mechanism in their target cells. *Cell.* 47:929–937.

Bender, A., and G. F. Sprague, Jr. 1989. Pheromones and pheromone receptors are the primary determinants of mating specificity in the yeast Saccharomyces cerevisiae. *Genetics.* 121:463–476.

Benito, B., E. Moreno, and R. Losario. 1991. Half-life of plasma membrane ATPase and its activating system in resting yeast cells. *Biochim. Biophys. Acta.* 1063:265–268.

Benovic, J. L., M. Bouvier, M. G. Caron, and R. J. Lefkowitz. 1988. Regulation of adenylyl cyclase-coupled β-adrenergic receptors. *Annu. Rev. Cell Biol.* 4:405-428.

Boeke, J. D., F. LaCroute, and G. R. Fink. 1984. A positive selection for mutants lacking orotidine-5'-phosphate decarboxylase activity in yeast: 5-fluoro-orotic acid resistance. *Mol. Gen. Genet.* 197:345–346.

Bucci, C., R. G. Parton, I. H. Mather, H. Stunnenberg, K. Simons, B. Hoflack, and M. Zerial. 1992. The small GTPase rab5 functions as a regulatory factor in the early endocytic pathway. *Cell.* 70:715–728.

Carpenter, G., and S. Cohen. 1976. ^{125}I-labeled human epidermal growth factor: binding, internalization, and degradation in human fibroblasts. *J. Cell Biol.* 71:159–171.

Chavrier, P., R. G. Parton, H. P. Hauri, K. Simons, and M. Zerail. 1990. Localization of low molecular weight GTP binding proteins to exocytic and endocytic compartments. *Cell.* 62:317–329.

Chvatchko, Y., I. Howald, and H. Riezman. 1986. Two yeast mutants defective in endocytosis are defective in pheromone response. *Cell.* 46:355–364.

Clark, K. L., N. G. Davis, D. K. Wiest, J.-J. Hwang-Shum, and G. F. Sprague, Jr. 1988. Response of yeast α cells to a-factor pheromone: topology of the receptor and identification of a component of the response pathway. *Cold Spring Harbor Symp. Quant. Biol.* 53:611–620.

Dietzel, C., and J. Kurjan. 1987. The yeast *SCG1* gene: a Gα-like protein implicated in the a- and α-factor response pathway. *Cell.* 50:1001–1010.

Dohlman, H. G., J. Thorner, M. G. Caron, and R. J. Lefkowitz. 1991. Model systems for the study of seven-transmembrane-segment receptors. *Annu. Rev. Biochem.* 60:653–688.

Evan, G. I., G. K. Lewis, G. Ramsay, and J. M. Bishop. 1985. Isolation of monoclonal antibodies specific for human c-*myc* proto-oncogene product. *Mol. Cell. Biol.* 5:3610–3616.

Goldstein, J. L., M. S. Brown, R. G. Anderson, D. W. Russell, and W. J. Schneider. 1985. Receptor-mediated endocytosis: concepts emerging from the LDL Receptor System. *Annu. Rev. Cell Biol.* 1:1–39.

Griffiths, G., and J. Gruenberg. 1991. The arguments for pre-existing early and late endosomes. *Trends Cell Biol.* 1:5–9.

Griffiths, G., B. Hoflack, K. Simons, I. Mellman, and S. Kornfeld. 1988. The mannose 6-phosphate receptor and the biogenesis of lysosomes. *Cell.* 52: 329–341.

Gruenberg, J., and K. E. Howell. 1989. Membrane traffic in endocytosis: insights from cell-free assays. *Annu. Rev. Cell Biol.* 5:453–481.

Hagen, D. C., G. McCaffrey, and G. F. Sprague, Jr. 1986. Evidence the yeast *STE3* encodes a receptor for the peptide pheromone a factor: Gene sequence and implications for the structure of the presumed receptor. *Proc. Natl. Acad. Sci. USA.* 83:1418–1422.

Herskowitz, I. 1989. A regulatory hierarchy for cell specialization in yeast. *Nature (Lond.).* 342:749–757.

Jackson, C. L., and L. H. Hartwell. 1990*a*. Courtship in S. cerevisiae: both cell types choose mating partners by responding to the strongest pheromone signal. *Cell.* 63:1039–1051.

Jackson, C. L., and L. H. Hartwell. 1990*b*. Courtship in *Saccharomyces cerevisiae*: an early cell-cell interaction during mating. *Mol. Cell. Biol.* 10:2202–2213.

Jenness, D. D., and P. Spatrick. 1986. Down regulation of the α-factor pheromone receptor in S. cerevisiae. *Cell.* 46:345–353.

Jensen, R. E., and I. Herskowitz. 1984. Directionality and regulation of cassette substitution in yeast. *Cold Spring Harbor Symp. Quant. Biol.* 49:97–104.

Kassir, Y., and G. Simchen. 1976. Regulation of mating and meiosis in yeast by the mating-type region. *Genetics.* 82:187–206.

Konopka, J. B., D. D. Jenness, and L. H. Hartwell. 1988. The C-terminus of the S. cerevisiae α-pheromone receptor mediates an adaptive response to pheromone. *Cell.* 54:609–620.

Kornfeld, S., and I. Mellman. 1989. The biogenesis of lysosomes. *Annu. Rev. Cell Biol.* 5:483–525.

Kuchler, K., R. E. Sterne, and J. Thorner. 1989. *Saccharomyces cerevisiae STE6* gene product: a novel pathway for protein export in eukaryotic cells. *EMBO (Eur. Mol. Biol. Organ.) J.* 8:3973–3984.

Lemmon, S. K., and E. W. Jones. 1987. Clathrin requirement for normal growth of yeast. *Science (Wash. DC).* 238:504–509.

Maxfield, F. R., J. Schlessinger, Y. Schechter, I. Pastan, and M. C. Willingham. 1978. Collection of insulin, EGF and α_2-macroglobulin in the same patches on the surface of cultured fibroblasts and common internalization. *Cell.* 14:805–810.

Michaelis, S., and I. Herskowitz. 1988. The a-factor pheromone of *Saccharomyces cerevisiae* is essential for mating. *Mol. Cell. Biol.* 8:1309–1318.

Miyajima, I., M. Nakafuku, N. Nakayama, C. Brenner, A. Miyajima, K. Kaibuchi, K. Arai, Y. Kaziro, and K. Matsumoto. 1987. *GPA1*, a haploid-specific essential gene, encodes a yeast homolog of mammalian G protein which may be involved in mating factor signal transduction. *Cell.* 50: 1011–1019.

Moir, D., S. E. Stewart, B. C. Osmond, and D. Botstein. 1982. Cold-sensitive cell-division-cycle mutants of yeast: isolation, properties and pseudoreversion studies. *Genetics.* 100:547–563.

Novick, P., and R. Schekman. 1979. Secretion and cell-surface growth are blocked in a temperature-sensitive mutant of *Saccharomyces cerevisiae*. *Proc. Natl. Acad. Sci. USA.* 76:1858–1862.

Ohashi, A., J. Gibson, I. Gregor, and G. Schatz. 1982. Import of proteins into mitochondria: the precursor of cytochrome c_1 is processed in two steps, one of them heme-dependent. *J. Biol. Chem.* 257:13042–13047.

Payne, G. S., and R. Schekman. 1985. A test of clathrin function in protein secretion and cell growth. *Science (Wash. DC).* 230:1009–1014.

Payne, G. S., D. Baker, E. van Tuinen, and R. Schekman. 1988. Protein transport to the vacuole and receptor-mediated endocytosis by clathrin heavy chain-deficient *Saccharomyces cerevisiae*. *Mol. Cell. Biol.* 60:117–123.

Pearse, B. M. F., and M. S. Robinson. 1984. Purification and properties of 100 kd proteins from coated vesicles and their reconstitution with clathrin. *EMBO (Eur. Mol. Biol. Organ.) J.* 3:1951–1957.

Pfeffer, S. R. 1992. GTP-binding proteins in intracellular transport. *Trends Cell Biol.* 2:41–46.

Raths, S., J. Rohrer, F. Crausaz, and H. Riezman. 1993. *end3* and *end4*: two mutants defective in receptor-mediated and fluid-phase endocytosis in *Saccharomyces cerevisiae*. *J. Cell Biol.* 120:55–65.

Raymond, C. K., I. Howald-Stevenson, C. A. Vater, and T. H. Stevens. 1992. Morphological classification of the yeast vacuolar protein sorting mutants: evidence for a prevacuolar compartment in class E *vps* mutants. *Mol. Biol. Cell.* 3:1389–1402.

Reneke, J. E., K. J. Blumer, W. E. Courchesne, and J. Thorner. 1988. The carboxy-terminal segment of the yeast α-factor receptor is a regulatory domain. *Cell.* 55:221–234.

Roberts, C. J., G. Pohlig, J. H. Rothman, and T. H. Stevens. 1989. Structure, biosynthesis, and localization of dipeptidyl aminopeptidase B, an integral membrane glycoprotein of the yeast vacuole. *J. Cell Biol.* 108:1363–1373.

Roberts, C. J., C. K. Raymond, C. T. Yamashiro, and T. H. Stevens. 1991. Methods for studying the yeast vacuole. *In* Methods in Enzymology. Vol. 194. C. G. Guthrie and G. R. Fink, editors. Academic Press, Inc., 644–661.

Rothman, J. H., and T. H. Stevens. 1986. Protein sorting in yeast: mutants

defective in vacuole biogenesis mislocalize vacuolar proteins into the late secretory pathway. *Cell.* 47:1041–1051.

Rothman, J. H., C. P. Hunter, L. A. Valls, and T. H. Stevens. 1986. Overproduction-induced mislocalization of a yeast vacuolar protein allows isolation of its structural gene. *Proc. Natl. Acad. Sci. USA.* 83:3248–3252.

Rothstein, R. 1991. Targeting, disruption, replacement, and allele rescue: integrative DNA transformation in yeast. *In* Methods in Enzymology, Vol. 194. C. G. Guthrie and G. R. Fink, editors. Academic Press, Inc., 281–301.

Schlessinger, J. 1988. The epidermal growth factor receptor as a multifunctional allosteric protein. *Biochemistry.* 27:3119–3123.

Schlessinger, J., Y. Schecter, M. C. Willingham, and I. Pastan. 1978. Direct visualization of binding, aggregation, and internalization of insulin and epidermal growth factor on living fibroblastic cells. *Proc. Natl. Acad. Sci. USA.* 75:2659–2663.

Sikorski, R. S., and P. Hieter. 1989. A system of shuttle vectors and yeast host strains designed for efficient manipulation of DNA in *Saccharomyces cerevisiae*. *Genetics.* 122:19–27.

Siliciano, P., and K. Tatchell. 1984. Transcription and regulatory signals at the mating type locus in yeast. *Cell.* 37:969–978.

Singer, B., and H. Riezman. 1990. Detection of an intermediate compartment involved in transport of α-factor from the plasma membrane to the vacuole in yeast. *J. Cell Biol.* 110:1911–1922.

Stevens, T., B. Esmon, and R. Schekman. 1982. Early stages in the yeast secretory pathway are required for transport of carboxypeptidase Y to the vacuole. *Cell.* 30:439–448.

Stevenson, B. J., N. Rhodes, B. Errede, and G. F. Sprague, Jr. 1992. Constitutive mutants of the protein kinase STE11 activate the yeast pheromone response pathway in the absence of the G protein. *Genes & Dev.* 6:1293–1304.

Tatchell, K., K. A. Nasmyth, and B. D. Hall. 1981. In vitro mutation analysis of the mating-type locus in yeast. *Cell.* 27:25–35.

Trowbridge, I. S. 1991. Endocytosis and signals for internalization. *Curr. Opin. Cell Biol.* 3:634–641.

Trueheart, J. H., and G. R. Fink. 1989. The yeast cell fusion protein FUS1 is O-glycosylated and spans the plasma membrane. *Proc. Natl. Acad. Sci. USA.* 86:9916–9920.

van der Sluijs, P., M. Hull, A. Zahraoui, A. Tavitian, B. Goud, and I. Mellman. 1991. The small GTP-binding protein rab4 is associated with early endosomes. *Proc. Natl. Acad. Sci. USA.* 88:6313–6317.

van der Sluijs, P., M. Hull, P. Webster, P. Male, B. Goud, and I. Mellman. 1992. The small GTP-binding protein rab4 controls an early sorting event on the endocytic pathway. *Cell.* 70:729–740.

Whiteway, M., L. Hougan, D. Dignard, D. Y. Thomas, L. Bell, G. C. Saari, F. J. Grant, P. O'Hara, and V. L. MacKay. 1989. The *STE4* and *STE18* genes of yeast encode potential β and γ subunits of the mating factor receptor-coupled G protein. *Cell.* 56:467–477.

Whiteway, M., L. Hougan, and D. Y. Thomas. 1990. Overexpression of the *STE4* gene leads to mating response in haploid *Saccharomyces cerevisiae*. *Mol. Cell. Biol.* 10:217–222.

Wichmann, H., L. Hengst, and D. Gallwitz. 1992. Endocytosis in yeast: evidence for involvement of a small GTP-binding protein (Ypt7p). *Cell.* 71: 1131–1142.

Zanolari, B., S. Raths, B. Singer-Kruger, and H. Riezman. 1992. Yeast pheromone receptor endocytosis and hyperphosphorylation are independent of G protein-mediated signal transduction. *Cell.* 71:755–763.